

# Severe Zinc Depletion of *Escherichia coli*

## ROLES FOR HIGH AFFINITY ZINC BINDING BY *ZinT*, ZINC TRANSPORT AND ZINC-INDEPENDENT PROTEINS<sup>\*[5]</sup>

Received for publication, March 31, 2009 Published, JBC Papers in Press, April 19, 2009, DOI 10.1074/jbc.M109.001503

Alison I. Graham<sup>‡</sup>, Stuart Hunt<sup>‡</sup>, Sarah L. Stokes<sup>§</sup>, Neil Bramall<sup>§</sup>, Josephine Bunch<sup>§1</sup>, Alan G. Cox<sup>§</sup>, Cameron W. McLeod<sup>§</sup>, and Robert K. Poole<sup>‡2</sup>

From the <sup>‡</sup>Department of Molecular Biology and Biotechnology and the <sup>§</sup>Centre for Analytical Sciences, The University of Sheffield, Western Bank, Sheffield S10 2TN, United Kingdom

Zinc ions play indispensable roles in biological chemistry. However, bacteria have an impressive ability to acquire Zn<sup>2+</sup> from the environment, making it exceptionally difficult to achieve Zn<sup>2+</sup> deficiency, and so a comprehensive understanding of the importance of Zn<sup>2+</sup> has not been attained. Reduction of the Zn<sup>2+</sup> content of *Escherichia coli* growth medium to 60 nM or less is reported here for the first time, without recourse to chelators of poor specificity. Cells grown in Zn<sup>2+</sup>-deficient medium had a reduced growth rate and contained up to five times less cellular Zn<sup>2+</sup>. To understand global responses to Zn<sup>2+</sup> deficiency, microarray analysis was conducted of cells grown under Zn<sup>2+</sup>-replete and Zn<sup>2+</sup>-depleted conditions in chemostat cultures. Nine genes were up-regulated more than 2-fold ( $p < 0.05$ ) in cells from Zn<sup>2+</sup>-deficient chemostats, including *zinT* (*yodA*). *zinT* is shown to be regulated by Zur (zinc uptake regulator). A mutant lacking *zinT* displayed a growth defect and a 3-fold lowered cellular Zn<sup>2+</sup> level under Zn<sup>2+</sup> limitation. The purified ZinT protein possessed a single, high affinity metal-binding site that can accommodate Zn<sup>2+</sup> or Cd<sup>2+</sup>. A further up-regulated gene, *ykgM*, is believed to encode a non-Zn<sup>2+</sup> finger-containing paralogue of the Zn<sup>2+</sup> finger ribosomal protein L31. The gene encoding the periplasmic Zn<sup>2+</sup>-binding protein *znuA* showed increased expression. During both batch and chemostat growth, cells “found” more Zn<sup>2+</sup> than was originally added to the culture, presumably because of leaching from the culture vessel. Zn<sup>2+</sup> elimination is shown to be a more precise method of depleting Zn<sup>2+</sup> than by using the chelator *N,N,N',N'*-tetrakis(2-pyridylmethyl)ethylenediamine.

Almost all biological interactions depend upon contacts between precisely structured protein domains, and Zn<sup>2+</sup> may be used to facilitate correct folding and stabilize the domain (1, 2). Zn<sup>2+</sup> also plays an indispensable catalytic role in many proteins (1). Although normally classed as a trace element, Zn<sup>2+</sup> accumulates to the same levels as calcium and iron in the *Esch-*

*erichia coli* cell (3); predicted Zn<sup>2+</sup>-binding proteins account for 5–6% of the total proteome (4).

However, despite its indispensable role in biology, as with all metals, Zn<sup>2+</sup> can become toxic if accumulated to excess. With no subcellular compartments to deposit excess metal, Zn<sup>2+</sup> homeostasis in bacteria relies primarily on tightly regulated import and export mechanisms (5). The major inducible high affinity Zn<sup>2+</sup> uptake system is the ABC transporter ZnuABC. ZnuA is important for growth (6) and Zn<sup>2+</sup> uptake (7) and is thought to pass Zn<sup>2+</sup> to ZnuB for transport through the membrane. Zn<sup>2+</sup>-bound Zur represses transcription of *znuABC*, whereas the addition of the metal chelator TPEN<sup>3</sup> de-represses expression from a promoterless *lacZ* gene inserted into *znuA*, *znuB*, and *znuC* (8). Zur can sense subfemtomolar concentrations of cytosolic Zn<sup>2+</sup>, implying that cellular Zn<sup>2+</sup> starvation commences at exceptionally low Zn<sup>2+</sup> concentrations (3). Outten and O'Halloran (3) found that the minimal Zn<sup>2+</sup> content required for growth in *E. coli* is  $2 \times 10^5$  atoms/cell, which corresponds to a total cellular Zn<sup>2+</sup> concentration of 0.2 mM, ~2000 times the Zn<sup>2+</sup> concentration found in the medium. A similar cellular concentration of Zn<sup>2+</sup> was found in cells grown in LB medium.

Thus, *E. coli* has an impressive ability to acquire and concentrate Zn<sup>2+</sup> (3), making the task of depleting this organism of Zn<sup>2+</sup> very difficult. Nevertheless, during the course of this work, a paper was published (9) in which the authors conclude that ZinT (formerly YodA) “is involved in periplasmic zinc binding and either the subsequent import or shuttling of zinc to periplasmic zinc-containing proteins under zinc-limiting conditions.” Surprisingly, this conclusion was drawn from experiments in which Zn<sup>2+</sup> levels in the medium were lowered only by reducing the amount of Zn<sup>2+</sup> added, without metal extraction or chelation.

Only a few attempts have been made to study the global consequences of metal deficiency using “omic” technologies. A study using TPEN (10) found 101 genes to be differentially regulated in *E. coli*. However, the authors note that TPEN has been reported to bind Cd<sup>2+</sup>, Co<sup>2+</sup>, Ni<sup>2+</sup>, and Cu<sup>2+</sup> more tightly than it binds Zn<sup>2+</sup>, and indeed, 34 of the 101 differentially regulated

\* This work was supported by the Biotechnology and Biological Sciences Research Council, UK.

[5] The on-line version of this article (available at <http://www.jbc.org>) contains supplemental Tables S1 and S2 and Fig. S1.

<sup>1</sup> Present address: School of Chemistry, University of Birmingham, Edgbaston, Birmingham B15 2TT, UK.

<sup>2</sup> To whom correspondence should be addressed: Dept. of Molecular Biology and Biotechnology, The University of Sheffield, Western Bank, Sheffield S10 2TN, UK. Tel.: 114-222-4447; Fax: 114-222-2800; E-mail [r.poole@sheffield.ac.uk](mailto:r.poole@sheffield.ac.uk).

<sup>3</sup> The abbreviations used are: TPEN, *N,N,N',N'*-tetrakis(2-pyridylmethyl)ethylenediamine; ICP-AES, inductively coupled plasma-atomic emission spectroscopy; LOD, limit of detection; MES, 2-(*N*-morpholino)ethanesulfonic acid; MF, mag-fura-2; PTFE, polytetrafluoroethylene (Teflon®); qRT, quantitative real time; GGM, glycerol-glycerophosphate medium; MOPS, 4-morpholinepropanesulfonic acid.

## Transcriptional Response to Zinc Limitation

**TABLE 1**  
List of strains used

Strain	Genotype	Source
AL6	MC4100 $\lambda\Phi(P_{zinT}-lacZ)$	Ref. 25
FB20133	MG1655 <i>ykgM::kan</i>	University of Wisconsin Genome Project
FB23354	MG1655 <i>znuA::kan</i>	University of Wisconsin Genome Project
MC4100	F <sup>-</sup> <i>araD139</i> $\Delta$ ( <i>argF-lac</i> )U169 <i>rpsL150 relA1 flbB5301 deoC1 ptsF25 rbsR</i>	Ref. 25
MG1655	F <sup>-</sup> $\lambda^{-}$ <i>ilvG rfb-50 rph-1</i>	Laboratory stock
SIP812	MC4100 <i>zur::Spc<sup>r</sup></i>	Ref. 8
RKP5082	MG1655/pKD46 (Amp <sup>r</sup> )	This work
RKP5456	MG1655 <i>zinT::cam</i>	This work
RKP5466	BL21(DE3) pLysS pET28a- <i>zinT</i>	This work
RKP5475	AL6 with <i>zur::Spc<sup>r</sup></i>	This work

genes are transcriptionally regulated by Fur (the iron (Fe) uptake regulator) or involved in iron or copper metabolism. Thus, the transcriptome of *E. coli* associated with Zn<sup>2+</sup> deficiency alone has not been elucidated. Most genome-wide microarray studies of the effects of metal stresses to date have been carried out in batch culture, but continuous culture offers major benefits for such studies. The greater biological homogeneity of continuous cultures and the ability to control all of the relevant growth conditions, such as pH and especially growth rate, eliminate the masking effects of secondary stresses and growth rate changes, allowing more precise delineation of the response to an individual stress (11, 12). In the case of transcriptomics, it has been demonstrated that the reproducibility of analyses between different laboratories is greater when chemostat cultures are used than when identical analyses are performed with batch cultures (13). Some studies have exploited continuous culture to examine the effects of metal stresses, such as that of Lee *et al.* (14) in which *E. coli* cultures grown in continuous culture at a fixed specific growth rate, temperature, and pH were used to assay the transcriptional response to Zn<sup>2+</sup> excess. In the present study, *E. coli* was grown in continuous culture in which severe depletion was achieved without recourse to chelating agents in the medium by thorough extraction and scrupulous attention to metal contamination. Microarray analysis identifies only nine genes that respond significantly to Zn<sup>2+</sup> starvation. We demonstrate here for the first time that one such gene, *zinT*, is up-regulated in response to extreme Zn<sup>2+</sup> deprivation by Zur and that ZinT has a high affinity for Zn<sup>2+</sup>. We also reveal roles for Zn<sup>2+</sup> redistribution in surviving Zn<sup>2+</sup> deficiency.

### EXPERIMENTAL PROCEDURES

**Bacterial Strains and Growth Conditions**—Bacterial strains used in this study are listed in Table 1. The cells were grown in glycerol-glycerophosphate medium (GGM), slightly modified from Beard *et al.* (15). GGM is buffered with MES, which has minimal metal chelating properties, and uses organic phosphate as the phosphate source to minimize formation of insoluble metal phosphates (16). The final concentrations are: MES (40.0 mM), NH<sub>4</sub>Cl (18.7 mM), KCl (13.4 mM),  $\beta$ -glycerophosphate (7.64 mM), glycerol (5.00 mM), K<sub>2</sub>SO<sub>4</sub> (4.99 mM), MgCl<sub>2</sub> (1.00 mM), EDTA (134  $\mu$ M), CaCl<sub>2</sub>·2H<sub>2</sub>O (68.0  $\mu$ M), FeCl<sub>3</sub>·6H<sub>2</sub>O (18.5  $\mu$ M), ZnO (6.14  $\mu$ M), H<sub>3</sub>BO<sub>3</sub> (1.62  $\mu$ M), CuCl<sub>2</sub>·2H<sub>2</sub>O (587 nM), Co(NO<sub>3</sub>)<sub>2</sub>·6H<sub>2</sub>O (344 nM), and (NH<sub>4</sub>)<sub>6</sub>Mo<sub>7</sub>O<sub>24</sub>·4H<sub>2</sub>O (80.9 nM) in MilliQ water (Millipore). Bulk elements (MES, NH<sub>4</sub>Cl,

KCl, K<sub>2</sub>SO<sub>4</sub>, and glycerol in MilliQ water at pH 7.4 (batch growth) or 7.6 (continuous culture)) were passed through a column containing Chelex-100 ion exchange resin (Bio-Rad) to remove contaminating cations. Trace elements (with or without Zn<sup>2+</sup> as necessary) and a CaCl<sub>2</sub> solution were then added to give the final concentrations shown above prior to autoclaving. After autoclaving, MgCl<sub>2</sub> and  $\beta$ -glycerophosphate were added at the final concentrations shown. All of the chemicals were of AnalaR grade purity or higher. Chelex-100 was packed into a Bio-Rad Glass Econo-column (~120 × 25 mm) that had previously been soaked in 3.5% nitric acid for 5 days.

**Creating Zn<sup>2+</sup>-deficient Conditions and Establishing Zn<sup>2+</sup>-limited Cultures**—Culture vessels and medium were depleted of Zn<sup>2+</sup> by extensive acid washing of glassware, the use of a chemically defined minimal growth medium, chelation of contaminating cations from this medium using Chelex-100, and the use of newly purchased high purity chemicals and metal-free pipette tips. Plastics that came into contact with the medium (*e.g.* bottles, tubes, and tubing) were selected on the basis of their composition and propensity for metal leaching, and included polypropylene, polyethylene, polytetrafluoroethylene (PTFE), or polyvinyl chloride. Dedicated weigh boats, spatulas, measuring cylinders, PTFE-coated stir bars, and a pH electrode were used. PTFE face masks, polyethylene gloves, and a PTFE-coated thermometer were also used. The solutions were filter-sterilized using polypropylene syringes with no rubber seal, in conjunction with syringe filters with a PTFE membrane and polypropylene housing. Vent filters contained a PTFE membrane in polypropylene housing. The cells were grown in continuous culture in a chemostat that was constructed entirely of nonmetal parts as detailed below.

**Continuous Culture of *E. coli* Strain MG1655**—*E. coli* strain MG1655 was grown in custom-built chemostats made entirely of nonmetal parts essentially as described by Lee *et al.* (14) with some modifications. Glass growth vessels and flow-back traps were soaked extensively (approximately two months) in 10% nitric acid before rinsing thoroughly in MilliQ water. Vent filters (Vent Acro 50 from VWR) were connected to the vessel using PTFE tubing. Metal-free pipette tips were used (MAXYMum Recovery Filter Tips from Axygen). Culture volume was maintained at 120 ml using an overflow weir in the chemostat vessel (14). The vessel was inoculated using one of the side arms. Flasks were stirred on KMO 2 Basic IKA-Werke stirrers at 437 rpm determined using a handheld laser tachometer (Compact Instruments Ltd). The use of a vortex impeller suspended from above the culture avoided grinding of the glass vessel that would occur if a stir bar were used. The samples were taken from the culture vessel as in Lee *et al.* (14). The dilution rate (and hence the specific growth rate) was 0.1 h<sup>-1</sup> (which is below the maximal specific growth rate  $\mu_{max}$  for this strain (17)). No washout was observed in long term chemostat cultures in Zn<sup>2+</sup>-depleted medium. One chemostat was fed medium that contained “adequate” Zn<sup>2+</sup> (*i.e.* normal GGM concentration), whereas the other contained no added Zn<sup>2+</sup> and had been depleted of Zn<sup>2+</sup> as above. Chemostats were grown for 50 h to allow five culture volumes to pass through the vessel and allow an apparent (pseudo-)steady state to be reached. More prolonged growth was avoided to minimize the

formation of mutations in the *rpoS* gene (18). Samples were taken throughout to check pH,  $A_{600}$ , glycerol content and for contaminants. Steady state values for pH and  $A_{600}$  were 6.9 and 0.6, respectively. Glycerol assays (19) showed cultures to be glycerol-limited.

The  $Zn^{2+}$ -free chemostat was inoculated with cells that had been subcultured in  $Zn^{2+}$ -free medium. A 0.25-ml aliquot of a saturated culture of strain MG1655 grown in LB was centrifuged, and the pellet was used to inoculate 5 ml of GGM that was incubated overnight at 37 °C with shaking. A 2.4-ml (*i.e.* 2% of chemostat volume) aliquot of this was then used to inoculate the chemostat. The adequate  $Zn^{2+}$  chemostat was inoculated with cells treated in essentially the same way but grown in GGM containing adequate  $Zn^{2+}$ . The two cultures ( $\pm Zn^{2+}$ ) used to inoculate the chemostats had  $A_{600}$  readings within 2.5% of each other. Aliquots from the chemostat were used to harvest RNA and for metal analysis by inductively coupled plasma-atomic emission spectroscopy (ICP-AES; see below).

**Batch Growth of *E. coli* Strains in GGM  $\pm Zn^{2+}$** —A saturated culture was grown in LB (with antibiotics as appropriate). To minimize carry-over of broth, the cells were collected from ~0.25 ml of culture by centrifugation, and the pellet was resuspended in a 5-ml GGM starter culture (with  $Zn^{2+}$  and antibiotics as appropriate) for 24 h. Side arm flasks containing 25 ml GGM with  $Zn^{2+}$  were then inoculated with the equivalent of 1 ml of a culture with  $A_{600}$  of 0.6. For these experiments, cultures with zinc were grown in medium containing adequate  $Zn^{2+}$  where no special precautions were taken in preparing the medium. Zinc-depleted cultures were grown in side arm flasks that had been soaked extensively in 10% nitric acid before being rinsed thoroughly in MilliQ water. Growth was measured over several hours using a Klett colorimeter and a red filter (number 66; Manostat Corporation). The colorimeter was blanked using GGM. No antibiotics were present in the growth medium used for batch growth curves because they can act as chelators (20–23), but cultures were spotted onto solid LB plates with and without antibiotics at the end of the growth curve to verify that antibiotic resistance was retained. At the end of the growth curve, aliquots of the culture were combined and pelleted for ICP-AES analysis (see below).

**RNA Isolation and Microarray Procedures**—These were conducted as described by Lee *et al.* (14). RNA was quantified using a BioPhotometer (Eppendorf). *E. coli* K-12 V2 OciChip microarray slides were purchased from Ocimum Biosolutions Ltd. (previously MWG Biotech). Biological experiments (*i.e.* comparison of low  $Zn^{2+}$  versus adequate  $Zn^{2+}$  in chemostat culture) were carried out three times, and a dye swap was performed for each experiment, providing two technical repeats for each of the three biological repeats. The data were analyzed as before (14). Spots automatically flagged as bad, negative, or poor in the Imagen software were removed before the statistical analysis was carried out in GeneSight.

***zinT* Gene Inactivation**—The *zinT* gene was functionally inactivated by the insertion of a chloramphenicol resistance cassette using the method of Datsenko and Wanner (24). The pACYC184 chloramphenicol resistance cassette was amplified by PCR using primers that have 40 bases of identity at their 5' ends to regions within the *zinT* gene. The forward primer was

5'-GCATGGTCATCACTCACACGGCAAACCCCTTAACA-GAGGTCAAGCCACTGGAGCACCTCAA-3' and the reverse was 5'-CAATGCCGTCTCAATGCCAATCATCTCG-ATATCTGTTGCACGGGGAGAGCCTGAGCAA-3' (the regions homologous to *zinT* are underlined). The linear DNA was used to transform strain RKP5082 by electroporation. This strain contains pKD46, which overexpresses the phage  $\lambda$  recombination enzymes when arabinose is present. Bacteria were grown to an  $A_{600}$  of 0.6 in 500 ml of LB containing ampicillin (final concentration, 150  $\mu$ g/ml) and arabinose (final concentration, 1 mM) at 30 °C. The cells were then pelleted and made electrocompetent by washing the pellet three times in ice-cold 10% glycerol. The last pellet was not resuspended but vortexed into a slurry. Aliquots of cells (50–100  $\mu$ l) were electroporated with 1–10% linear DNA (v/v) at 1800 V. The cells were recovered by the addition of 1 ml of LB and incubation at 37 °C for 90 min. The cells were then pelleted and plated onto LB containing chloramphenicol at 34  $\mu$ g/ml (final concentration). Loss of pKD46 plasmid was checked by streaking transformants on LB agar plates containing ampicillin (final concentration, 150  $\mu$ g/ml). Insertion of the chloramphenicol cassette was checked by DNA sequencing. The *zinT::cam* (chloramphenicol resistance cassette) mutant strain was named RKP5456.

**Construction of a  $\lambda\Phi(P_{zinT-lacZ})$  *zur::Spc<sup>r</sup>* Strain**—The *zur::Spc<sup>r</sup>* (spectinomycin resistance cassette) mutation in strain SIP812 (8) was moved into strain AL6, which harbors the  $\lambda\Phi(P_{zinT-lacZ})$  fusion (25), by P1 transduction (26). The strain was named RKP5475.

**Quantitative Real Time (*qRT*)-PCR**—This was carried out on RNA samples harvested from the chemostats exactly as described in Lee *et al.* (14). The mRNA levels of *holB* were unchanged as determined by array analysis and were thus used as an internal control.

**ICP-AES**—Cells (from 25 ml (batch) or ~85 ml of culture (chemostat)) were harvested by centrifugation at 5000  $\times g$  for 5 min (Sigma 4K15) in polypropylene tubes from Sarstedt (catalogue numbers 62.547.004 (50 ml) or 62.554.001 (15 ml)). Culture supernatants were retained for analysis. The pellets were washed three times in 0.5 ml of 0.5%  $HNO_3$  (Aristar nitric acid, 69% v/v) to remove loosely bound elements. Supernatants collected from the washes were also retained for analysis.

The pellets were resuspended in 0.5 ml of  $HNO_3$  (69%) before transfer to nitric acid-washed test tubes (previously dried). The samples were placed in an ultrasonic bath for ~30 min to break the cells. The resultant digest was then quantitatively transferred to a calibrated 15-ml tube and made up to 5 ml with 1%  $HNO_3$ . The samples were analyzed using a Spectrociros<sup>CCD</sup> (Spectroanalytical) inductively coupled plasma-atomic emission spectrometer using background correction. Analyte curves were created for each element to be tested using multi-element standard solutions containing 0.1, 0.2, 1, 5, and 10 mg liter<sup>-1</sup>. The wavelengths (nm) for each element were as follows: calcium, 183.801; cobalt, 228.616; copper, 324.754 and 327.396; iron, 259.941; magnesium, 279.079; molybdenum, 202.030; sodium, 589.592; and zinc, 213.856. A 1% nitric acid solution in MilliQ water was used as a blank and to dilute cell digests before ICP-AES analysis. Concentrations of each element in each sam-

## Transcriptional Response to Zinc Limitation

ple (pellets, culture supernatants, and wash supernatants) were calculated using the standard curves. The measurements obtained were the means of five replicate integrations. The limit of  $Zn^{2+}$  detection was  $0.001 \text{ mg liter}^{-1}$  (*i.e.* 1 ppb). In the "simple" low matrix solutions analyzed here, the wavelength used for  $Zn^{2+}$  detection is interference-free and specific for  $Zn^{2+}$ .

Elemental recoveries were calculated from these samples. Two different recovery calculations were performed: 1) the percentage of an element in the culture that was subsequently recovered in the washed cell pellet, wash supernatants, and culture supernatant, and 2) the percentage of an element recovered in the unwashed pellet and culture supernatant. The former was used for batch and chemostat samples, and the latter was used for chemostat only. In some samples, element concentrations were below the calculated limit of detection (LOD) for the method. LOD is calculated from the calibration curve based on three  $\sigma$  of a blank signal. Where the signal is at or below the LOD, the instrument reports a <LOD value. In these cases, the LOD is used in subsequent calculations, so it will be an overestimation. Detection of  $Zn^{2+}$  was further complicated because, in many cases,  $Zn^{2+}$  concentrations were close to unavoidable background levels.

**Calculation of Dry Cell Weight**—Cellular metal contents were expressed on a dry cell mass basis. This was determined by filtering known volumes of culture (10, 20, and 30 ml) through preweighed cellulose nitrate filters (47-mm diameter and pore size of  $0.2 \mu\text{m}$ ; Millipore). The filters had previously been dried at  $105^\circ\text{C}$  for 18–24 h to constant weight. The filters were again dried at  $105^\circ\text{C}$  until a constant weight was attained, which was recorded.

**$\beta$ -Galactosidase Activity Assay**—For  $\beta$ -galactosidase assays with strains AL6 ( $\lambda\Phi(P_{zinT}\text{-lacZ})$ ) and RKP5475, a saturated culture was grown in LB with or without spectinomycin (final concentration,  $50 \mu\text{g/ml}$ ) as appropriate, and cells from  $\sim 0.25$  ml of culture were collected and resuspended in 5 ml GGM with or without  $Zn^{2+}$  and spectinomycin as appropriate. This was incubated overnight at  $37^\circ\text{C}$  with shaking. A 1-ml aliquot of this was then used to inoculate several cultures (15 ml) as described in the text. The cultures were harvested when an  $A_{600}$  of 0.2–0.4 was reached. Immediately prior to harvesting,  $5 \mu\text{l}$  was spotted onto solid LB plates with and without antibiotics to check that resistance was retained. Separate flasks were set up and used to grow the strains under each of the conditions mentioned above for ICP-AES analysis.

$\beta$ -Galactosidase activity was measured in  $\text{CHCl}_3$ - and SDS-permeabilized cells by monitoring the hydrolysis of *o*-nitrophenyl- $\beta$ -D-galactopyranoside. Cell pellets were resuspended in  $\sim 15$  ml of Z buffer (26). Each culture was assayed in triplicate. Absorbance (*A*) at 420, 550, and 600 nm was measured to allow  $\beta$ -galactosidase activity (Miller units) to be calculated as described in Ref. 26.

**Cloning of *zinT* for Protein Purification**—Primers 5'-CTCC-TGCCTTCATATGGGTCATCAC-3' (forward) and 5'-CAT-AGTGATGAGCTCGTCTGTAGC-3' (reverse) were used to amplify the *zinT* coding region minus the sequence that encodes the 24-amino acid periplasmic signaling sequence (27) from MG1655 genomic DNA. An NdeI site was engineered into

the forward primer and a SacI site into the reverse primer (underlined above), which, following enzymic digestion, allowed the 684-bp product to be ligated into pET28a (Novagen). The translated protein is produced with an N-terminal His tag and thrombin cleavage site. This allowed the protein to be purified using TALON metal affinity resin (Clontech), which uses immobilized  $\text{Co}^{2+}$  ions to trap polyhistidine tags with high affinity, followed by cleavage with thrombin to release the pure protein. Insertion of the correct fragment was verified by digestion with restriction endonucleases. pET28a containing the *zinT* gene fragment (pET28a-*zinT*) was used to transform *E. coli* overexpression strain BL21(DE3) pLysS and named strain RKP5466.

**Overexpression and Purification of Recombinant ZinT**—Strain RKP5466 was grown in LB containing kanamycin ( $50 \mu\text{g/ml}$ , to maintain pET28a-*zinT*) and chloramphenicol ( $34 \mu\text{g/ml}$ , to maintain pLysS) at  $37^\circ\text{C}$  with shaking to an  $A_{600}$  of 0.6, at which point isopropyl  $\beta$ -D-thiogalactopyranoside was added to a final concentration of 1 mM. The cells were harvested after a further 4 h of incubation. The pellets were stored at  $-80^\circ\text{C}$  for later use; a cell pellet derived from 1 liter of culture was resuspended in  $\sim 15$  ml of buffer P (50 mM Tris/MOPS, 100 mM KCl, pH 8) and sonicated on ice to break the cells. Cell debris was pelleted by centrifugation for 30 min at  $12\,000 \times g$  at  $4^\circ\text{C}$ , whereupon the supernatant was removed and further centrifuged for 15 min at  $27\,000 \times g$ . The cleared lysate was then loaded into a 5-ml TALON resin column, washed with 50 ml of buffer P, followed by 50 ml of buffer P containing 20 mM imidazole. Thrombin (60–80 units in 3–4 ml of buffer P) was pipetted onto the column, allowed to soak into the resin, and incubated overnight at room temperature. Ten 1-ml fractions were eluted using buffer P. Recombinant ZinT was determined to be  $>95\%$  pure by SDS-PAGE. Protein was quantified using its absorbance at 280 nm and the theoretical extinction coefficient of  $35995 \text{ M}^{-1} \text{ cm}^{-1}$  (estimated using the web-based program ProtParam at ExPASy), which assumes that all cysteines in the protein appear as half-cysteines using information based on (28). The theoretical extinction coefficient is based on the protein sequence minus the periplasmic targeting sequence.

**N-terminal Protein Sequencing**—Following SDS-PAGE, purified YodA was blotted onto a polyvinylidene fluoride membrane. The fragment of interest was excised from the membrane, and the sequence was determined using an Applied Biosystems Procise 392 protein sequencer.

**Assays of Metal Binding to Purified ZinT**—Purified recombinant ZinT was exchanged into buffer D (20 mM MOPS, pH 7) using a PD-10 desalting column (GE Healthcare). ZinT (1 ml) was incubated with various concentrations of  $\text{ZnSO}_4 \cdot 7\text{H}_2\text{O}$  (ACS grade reagent) and/or  $\text{CdCl}_2 \cdot 2\frac{1}{2}\text{H}_2\text{O}$  (AnalaR grade) for 1 h at room temperature. The protein/metal mixture was then loaded onto a PD-10 column and eluted in  $7 \times 0.5$ -ml fractions using buffer D. The fractions were assayed for  $A_{280}$  and for metal content using ICP-AES. Quantification of some elements was below the LOD in a limited number of samples that do not affect the overall interpretation of the experiment. In these cases the value for the LOD was used for subsequent calculations and thus will be an overestimation.

**TABLE 2**

Expected and representative measured amounts of elements in Zn<sup>2+</sup>-sufficient and -depleted GGM

Element	Predicted from medium composition	Measured by ICP-AES	
		Zn <sup>2+</sup> -sufficient	Zn <sup>2+</sup> -depleted
	mg liter <sup>-1</sup>	mg liter <sup>-1</sup>	
Zinc	0.401/0 (+zinc/-zinc)	0.340	0.004
Iron	1.045	0.886	0.878
Copper	0.037	0.033	0.034
Cobalt	0.0257	0.018	0.019
Molybdenum	0.054	0.068	0.059
Calcium	2.24	2.83	2.85
Magnesium	24.0	24.2	25.0

*Mag-fura-2 Binding Experiments*—Purified recombinant ZinT was exchanged into buffer M (140 mM NaCl, 20 mM Hepes, pH 7.4) using a PD-10 desalting column. Absorption spectra were collected using a Varian Cary 50 Bio UV-visible spectrophotometer at 37 °C. Buffer composition and experimental conditions were taken from Simons (47). ZinT (500 μl; ~15 μM) was placed in a quartz cuvette, and a spectrum was taken from which the concentration of ZinT was determined. Difference spectra were recorded in which the reference sample was buffer M. Equimolar mag-fura-2 (MF; Molecular Probes, catalogue number M-1290) was then added. Aliquots of ZnSO<sub>4</sub>·7H<sub>2</sub>O (ACS grade reagent) and/or CdCl<sub>2</sub>·2½H<sub>2</sub>O (AnalaR grade) in buffer M were added, mixed, and incubated for 1 min before the spectra were collected. The equilibrium was established within 1 min of Zn<sup>2+</sup> being added.

## RESULTS

*Creating Zn<sup>2+</sup>-deficient Conditions*—Several precautions, based on normal analytical practice and the findings of Kay (29) regarding Zn<sup>2+</sup> contamination, were taken to ensure that culture vessels and medium were depleted of Zn<sup>2+</sup> where necessary. Table 2 shows typical values for the amounts of various metals in GGM as analyzed by ICP-AES. Both Zn<sup>2+</sup>-depleted and -replete media show good correlation with the expected values. In various batches of media analyzed, Zn<sup>2+</sup> concentrations in Zn<sup>2+</sup>-depleted medium ranged from <0.001 to 0.004 mg liter<sup>-1</sup> (<15–60 nM Zn<sup>2+</sup>). The variation in Zn<sup>2+</sup> depletion achieved is a result of the difficulty in excluding Zn<sup>2+</sup> from all sources that come into contact with the medium and culture. Sodium was used as the exchanging ion on Chelex-100, but excess sodium was not detected in the medium following chelation (data not shown).

*Growth in Zn<sup>2+</sup>-depleted Batch Cultures*—*E. coli* strain MG1655 was grown in GGM with or without Zn<sup>2+</sup> (Fig. 1A). The Zn<sup>2+</sup>-limited culture showed a lag in entering the exponential phase, and a semi-logarithmic analysis of growth (not shown) revealed that the Zn<sup>2+</sup>-limited culture had an increased doubling time (159.0 min) compared with the Zn<sup>2+</sup>-replete culture (125.4 min) and reached a lower final *A* value. Because *A* measurements may reflect cell size changes (30), the samples were taken at the end of growth for electron microscopy, but no discernible size difference was seen between *E. coli* cells grown with or without Zn<sup>2+</sup> in GGM (not shown). Cells grown in GGM (±Zn<sup>2+</sup>) were, however, smaller (length, width, and volume) than cells grown in rich medium (LB), presumably because of a slower growth rate (31).

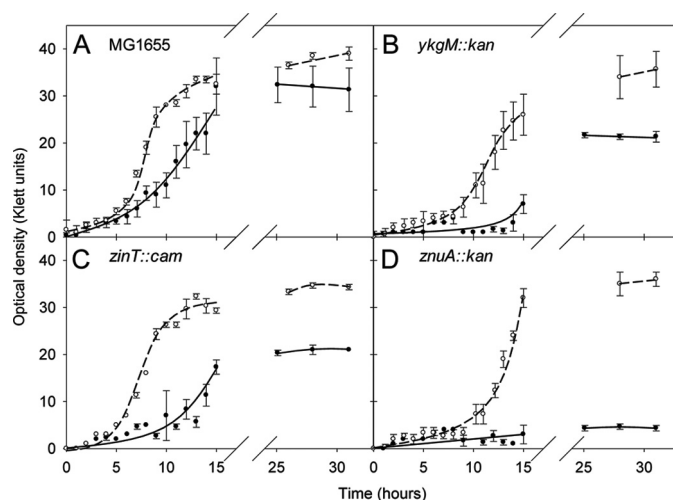


**FIGURE 1.** Growth of wild-type and isogenic mutant *E. coli* strains in Zn<sup>2+</sup>-depleted (filled circles, solid line) and Zn<sup>2+</sup>-replete (open circles, dashed line) GGM in batch culture. In each case, the means and standard deviations of three flasks are plotted. The doubling times of the strains during exponential growth, calculated from semi-logarithmic plots, were as follows: MG1655 replete, 125 min; MG1655 deplete, 159 min; *ykgM::kan* replete, 211 min; *ykgM::kan* deplete, 885 min; *zinT::cam* replete, 124 min; *zinT::cam* deplete, 193 min; *znuA::kan* replete 134 min; *znuA::kan* deplete, 492 min. A, MG1655 wild type; B, *ykgM::kan* (FB20133); C, *zinT::cam* (RKP5456); D, *znuA::kan* (FB23354).

GGM contains EDTA, which prevents precipitation of the trace elements present. This is a well established and common practice (17). However, to investigate whether this EDTA was itself creating Zn<sup>2+</sup> depletion, we cultured MG1655 in GGM with and without EDTA (supplemental Fig. S1). When grown in GGM without EDTA, MG1655 displayed a longer lag phase and reduced growth yield. The growth rate was also affected; the doubling time during exponential growth increased from 125.5 (with EDTA) to 131.5 min (without EDTA). Thus, EDTA is not creating a state of Zn<sup>2+</sup> depletion but rather is a beneficial component of the medium.

As well as growing at a reduced rate, cells grown in Zn<sup>2+</sup>-depleted medium had ~1.8–5.0-fold less cellular Zn<sup>2+</sup> than those grown in Zn<sup>2+</sup>-replete medium (based on three separate experiments). For example, at the end of the growth curve shown in Fig. 1A, the cells cultured in Zn<sup>2+</sup>-replete medium contained 1.12 × 10<sup>-5</sup> mg of Zn<sup>2+</sup>/mg of dry weight cells and the cells grown in Zn<sup>2+</sup>-depleted medium contained 3.40 × 10<sup>-6</sup> mg of Zn<sup>2+</sup>/mg of dry weight cells (a 3.3-fold difference). Here, “cellular Zn” is defined as that which cannot be removed by three successive washes with 0.5% nitric acid. To verify the reliability of the metal analyses, elemental recoveries were calculated from these samples. Fig. 2 shows that, for cells grown in Zn<sup>2+</sup>-replete medium, Zn<sup>2+</sup> recovery was between 90 and 110%, and for cells grown in Zn<sup>2+</sup>-replete and Zn<sup>2+</sup>-deplete medium, the recovery of iron, copper, cobalt, and magnesium was also between 90 and 110%. For these elements, therefore, the metal content in the washed pellet and the culture supernatant and the wash supernatants fully accounts for the metal initially added to the culture in the medium. However, this was not true for Zn<sup>2+</sup> recovery in cells grown in Zn<sup>2+</sup>-deficient medium. Zn<sup>2+</sup> in these cells, together with that in the culture supernatant and wash supernatants, was 5-fold higher than the amount originally added to the culture in the medium. This

## Transcriptional Response to Zinc Limitation

suggests an avid  $Zn^{2+}$  sequestering ability of cells cultured under limiting  $Zn^{2+}$  conditions. Details of the analyses of individual pellets, wash solutions, supernatants, and media for  $Zn^{2+}$  are found in [supplemental Table S1](#). We conclude that  $Zn^{2+}$  limitation can be achieved in batch culture without resorting to chelators despite effective bacterial  $Zn^{2+}$  scavenging mechanisms.

**Cells Grown in Continuous Culture “Find” Extra  $Zn^{2+}$** —To explore  $Zn^{2+}$  acquisition and localization at constant growth

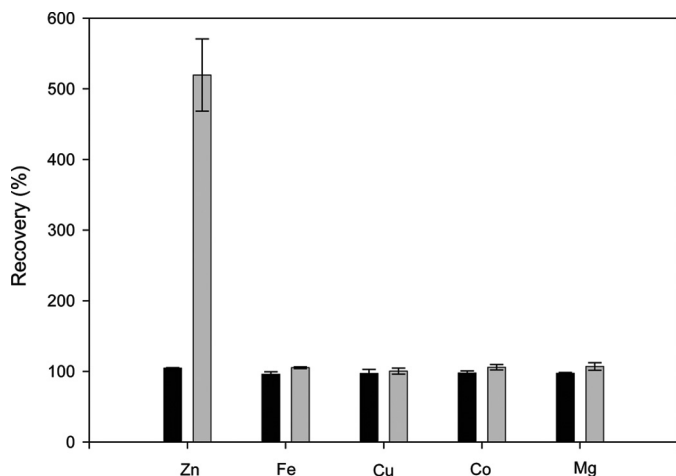


**FIGURE 2. Recovery of elements following growth of strain MG1655 in batch culture.** The means and standard deviations of three flasks are plotted. The black and gray bars represent the percentage of added elements recovered from cells grown in  $Zn^{2+}$ -replete and -deplete conditions, respectively. See text for details of calculation.

**TABLE 3**

**Recovery of  $Zn^{2+}$  from *E. coli* strain MG1655 growing in a  $Zn^{2+}$ -limited chemostat (Run 1) followed by successive cultures in the same chemostat under the same conditions (Runs 2–5)**

A run is an experiment conducted after terminating a chemostat experiment and re-establishing a new culture in the same apparatus. ND, not determined. See text for details of calculation.

Run	Recovery of $Zn^{2+}$ in medium			
	Washed cell pellet + wash solutions + supernatant		Unwashed cell pellet + supernatant	
	+Zinc	–Zinc	+Zinc	–Zinc
	%	%	%	%
1	104	1858	ND	ND
2	110	1676	ND	ND
3	105	559	ND	ND
4	104	493	102	454
5	103	248	103	254

**TABLE 4**

**Genes with a significant change in mRNA level in response to  $Zn^{2+}$  deficiency**

Only genes with a fold increase of more than 2 and a  $p$  value of less than 0.05 are included. The gene names are the primary names on Ecogene. The gene descriptions are from Ecogene.

Gene	b number	Gene product	Fold increase	$p$ value (<0.05)
<i>zinT</i>	b1973	Periplasmic cadmium-binding protein; induced by cadmium and peroxide; binds zinc, nickel, and cadmium; SoxS- and Fur-regulated	8.07	0.0001
<i>znuA</i>	b1857	High affinity ABC transport system for zinc, periplasmic	2.88	0.00117
<i>fdnG</i>	b1474	Formate dehydrogenase-N, selenopeptide, anaerobic; periplasmic	2.86	0.00386
<i>emtA</i>	b1193	Membrane-bound transglycosylase E, lipoprotein; involved in limited murein hydrolysis	2.86	0.00998
<i>ykgM</i>	b0296	RpmE paralogue, function unknown	2.64	0.03647
<i>mdtD</i>	b2077	Putative transporter, function unknown; no MDR phenotype when mutated or cloned; fourth gene in <i>mdtABCDBaeRS</i> operon	2.46	0.01614
<i>ribA</i>	b1277	GTP cyclohydrolase II, riboflavin biosynthesis	2.36	0.02506
<i>ydjE</i>	b1577	Pseudogene, N-terminal fragment, Qin prophage	2.17	0.00452
<i>aslA</i>	b3801	Suppresses <i>gpp</i> mutants; putative arylsulfatase	2.15	0.02660

rates and defined conditions for a detailed transcriptomic study, *E. coli* strain MG1655 was grown in parallel glycerol-limited chemostats, one fed with medium that contained “adequate”  $Zn^{2+}$  and one that had been rigorously depleted of  $Zn^{2+}$ . For the majority of elements assayed (iron, copper, cobalt, magnesium, molybdenum, potassium, sodium, phosphorus, and sulfur), the percentage recoveries were 90–110% (data not shown). However, more  $Zn^{2+}$  was recovered from the cells grown in the  $Zn^{2+}$ -deficient chemostat than was originally added to the culture (Table 3), as in batch culture (Fig. 2). This is presumed to be due to active leaching from glassware or carry-over from the inoculum. Interestingly, this percentage markedly decreased with successive experiments in the same chemostat apparatus, suggesting that there is less  $Zn^{2+}$  able to be leached after repeated runs of culture in the same chemostat vessel (Table 3). Details of the analyses of individual pellets, wash solutions, supernatants, and media are found in [supplemental Table S2](#).

Cells grown in the  $Zn^{2+}$ -deficient chemostat consistently contained less cellular  $Zn^{2+}$  than those grown in  $Zn^{2+}$ -replete medium (e.g.  $2.94 \times 10^{-5}$  mg of  $Zn^{2+}$ /mg of cells for cells grown in adequate  $Zn^{2+}$  and  $0.536 \times 10^{-5}$  mg of  $Zn^{2+}$ /mg of cells for cells harvested from run 5 of the  $Zn^{2+}$ -limited chemostat (a 5.5-fold decrease)).

**Transcriptome Changes Induced by  $Zn^{2+}$  Deficiency**—The genome-wide mRNA changes of strain MG1655 grown in continuous culture with adequate or limiting  $Zn^{2+}$  were probed using microarray technology. Commonly applied criteria to determine the significance in transcriptomic studies are a fold change of more than 2 and a  $p$  value of less than 0.05. Using these criteria, of the 4288 genes arrayed, only nine showed significant changes (an increase in all cases) in mRNA levels and are listed in Table 4. Genes not meeting these criteria may be biologically significant but are not studied further here. It should be noted that microarrays measure the relative abundance of mRNA but cannot inform as to whether changes occur because of changes in the rate of transcription or because of changes in the stability of the transcript.  $Zn^{2+}$  has been reported to affect the stability of the mRNA of a human  $Zn^{2+}$  transporter (32). The full data set has been deposited in GEO (accession number GSE11894) (33). Three genes were chosen for further study based on known links to  $Zn^{2+}$  homeostasis. The remaining six genes were not studied further. In total, 21 genes displayed a greater than 2-fold increase in mRNA levels,

TABLE 5

Changes in the mRNA levels from a number of genes in response to Zn<sup>2+</sup> deficiency

The gene names are the primary names on Ecogene. The gene descriptions are from Ecogene.

Gene	b number	Gene product	Fold change	p value
<i>yodB</i>	b1974	Function unknown	2.38	0.0725
<i>zur</i>	b4046	Repressor for <i>znuABC</i> , the zinc high affinity transport genes; dimer; binds two Zn(II) ions per monomer	1.37	0.9578
<i>znuC</i>	b1858	High affinity ABC transport system for zinc	1.36	0.2294
<i>znuB</i>	b1859	High affinity ABC transport system for zinc	1.34	<sup>a</sup>
<i>zntR</i>	b3292	Zinc-responsive activator of <i>zntA</i> transcription	1.34	0.4857
<i>zraS</i>	b4003	Two component sensor kinase for <i>ZraP</i> ; responsive to Zn <sup>2+</sup> and Pb <sup>2+</sup> ; autoregulated; regulation of Hyd-3 activity is probably due to cross-talk of overexpressed protein	1.32	0.1109
<i>zraP</i>	b4002	Zinc-binding periplasmic protein; responsive to Zn <sup>2+</sup> and Pb <sup>2+</sup> ; regulated by <i>zraSR</i> two-component system; rpoN-dependent	1.25	0.9322
<i>yjiP</i>	b3915	Iron and zinc efflux membrane transporter; cation diffusion facilitator family; dimeric	1.17	0.2742
<i>zitB</i>	b0752	Zn(II) efflux transporter; zinc-inducible	1.09	0.9571
<i>zntA</i>	b3469	Zn(II), Cd(II), and Pb(II) translocating P-type ATPase; mutant is hypersensitive to Zn <sup>2+</sup> and Cd <sup>2+</sup> salts	1.07	0.9285
<i>spy</i>	b1743	Periplasmic protein induced by zinc and envelope stress, part of <i>cpxR</i> and <i>baeSR</i> regulons	1.03	0.8314
<i>zraR</i>	b4004	Two component response regulator for <i>zraP</i> ; responsive to Zn <sup>2+</sup> and Pb <sup>2+</sup> ; autoregulated; regulation of Hyd-3 activity is probably due to cross-talk of overexpressed protein	0.95	0.9315
<i>zupT</i>	b3040	Zinc and other divalent cation uptake transporter	0.88	0.3258

<sup>a</sup> Insufficient data available to obtain a p value.

13 displayed a decrease, and the mRNA changes from 140 genes had a *p* value of <0.05. No genes exhibited a 2-fold or greater decrease in mRNA levels with a *p* value of less than 0.05.

The gene exhibiting the greatest change in transcription (and lowest *p* value) was *zinT* (up-regulated 8.07-fold), previously known as *yodA*. ZinT was initially identified in a global study of *E. coli* defective in the histone-like nucleoid-structuring protein H-NS (34). Levels of ZinT increase when cells are grown in the presence of Cd<sup>2+</sup> (27) and at pH 5.8 (35). More recently, it has been suggested that the abundance of *yodA* mRNA changes in response to cytoplasmic pH stress (36). Transcription of *zinT* is increased by the addition of Cd<sup>2+</sup>, but not Zn<sup>2+</sup>, Cu<sup>2+</sup>, Co<sup>2+</sup>, and Ni<sup>2+</sup>, to growing cells (25), even though Cd<sup>2+</sup>, Zn<sup>2+</sup>, and Ni<sup>2+</sup> were found in crystals of ZinT (37, 38) (see "Discussion"). Further evidence for the binding of Cd<sup>2+</sup> to ZinT was presented by Stojnev *et al.* (39), who found that  $\gamma$ -labeled <sup>109</sup>Cd<sup>2+</sup>-bound proteins could be detected in wild-type *E. coli* but not a mutant lacking *zinT* (39), suggesting a specific role for ZinT in Cd<sup>2+</sup> accumulation. ZinT is found primarily in the cytoplasm in unstressed cells but is exported to the periplasm upon Cd<sup>2+</sup> stress (25). The mature, periplasmic form of ZinT is thought to form a disulfide bond, because it is a substrate of DsbA (40). A recent paper (9) suggests a role for ZinT in periplasmic zinc binding under zinc-limiting conditions, but no direct evidence for *zinT* up-regulation in response to rigorous exclusion of zinc has been previously reported.

The *znuA* gene was also up-regulated in response to Zn<sup>2+</sup> depletion (Table 4). ZnuA is the soluble periplasmic metallochaperone component of the ZnuABC Zn<sup>2+</sup> importer and was up-regulated 2.88-fold. In this complex, ZnuB is the integral membrane protein, and ZnuC is the ATPase component. The *znuB* and *znuC* genes were up-regulated by 1.34- and 1.36-fold, respectively (with *p* values of >0.05 and thus are not shown in Table 4). No other genes that encode proteins involved in Zn<sup>2+</sup> transport (specifically *zupT*, *zur*, *zitB*, *zntA*, *zntR*, *zraS*, *zraR*, and *zraP*) were more than 1.4-fold up-regulated or 1.2-fold down-regulated, and all had *p* values of >0.05.

The changes in the mRNA levels of a number of genes involved in Zn<sup>2+</sup> metabolism are shown in Table 5.

The *ykgM* gene was up-regulated 2.64-fold in this study (Table 4) and has been identified previously by bioinformatics as the non-Zn<sup>2+</sup> ribbon-containing paralogue of the ribosomal protein L31 that normally contains a Zn<sup>2+</sup> ribbon motif and is thus predicted to bind Zn<sup>2+</sup> (41). Panina *et al.* (41) predicted (but did not show) that *ykgM* would be up-regulated upon Zn<sup>2+</sup> starvation and then displace the Zn<sup>2+</sup>-containing version of L31 in the ribosome, thus liberating Zn<sup>2+</sup> for use by Zn<sup>2+</sup>-containing enzymes. However, no previous study has attained the degree of Zn<sup>2+</sup> limitation reported here, and the role of *ykgM* has not been further explored.

To verify the results obtained by microarray experiments, several genes that were induced by Zn<sup>2+</sup> depletion were examined by qRT-PCR to determine independently relative mRNA levels. The levels of up-regulation determined by qRT-PCR (mean  $\pm$  normalized standard deviation) were as follows: *yodA*, 7.77  $\pm$  0.63; *ykgM*, 2.83  $\pm$  0.61; and *znuA*, 2.34  $\pm$  0.58. These values correspond closely to increases in the microarray analysis of 8.07-, 2.64-, and 2.88-fold, respectively. Similar qRT-PCR values were obtained on one (*ykgM* and *znuA*) or two (*yodA*) other occasions. The mRNA levels of *holB* (internal control) were unchanged as determined by qRT-PCR and array analysis.

*Hypersensitivity of Selected Strains to Zn<sup>2+</sup> Deficiency*—To assess the importance of the *ykgM*, *zinT*, and *znuA* genes in surviving Zn<sup>2+</sup> deficiency, mutants were used in which each gene are inactivated by insertion of an antibiotic resistance cassette; the growth of these isogenic strains was compared in Zn<sup>2+</sup>-depleted and Zn<sup>2+</sup>-replete liquid cultures (Fig. 1). Each strain (wild type and mutants) grew more poorly in the absence of Zn<sup>2+</sup> than in its presence. Also, in Zn<sup>2+</sup>-depleted medium, the *ykgM::kan* (kanamycin resistance cassette), *zinT::cam*, and *znuA::kan* mutants consistently grew more poorly than MG1655 in the same medium. We were unable to culture the *znuA::kan* mutant to >5 Klett units in the severely Zn<sup>2+</sup>-depleted conditions achieved here (Fig. 1D). All of the experi-

## Transcriptional Response to Zinc Limitation

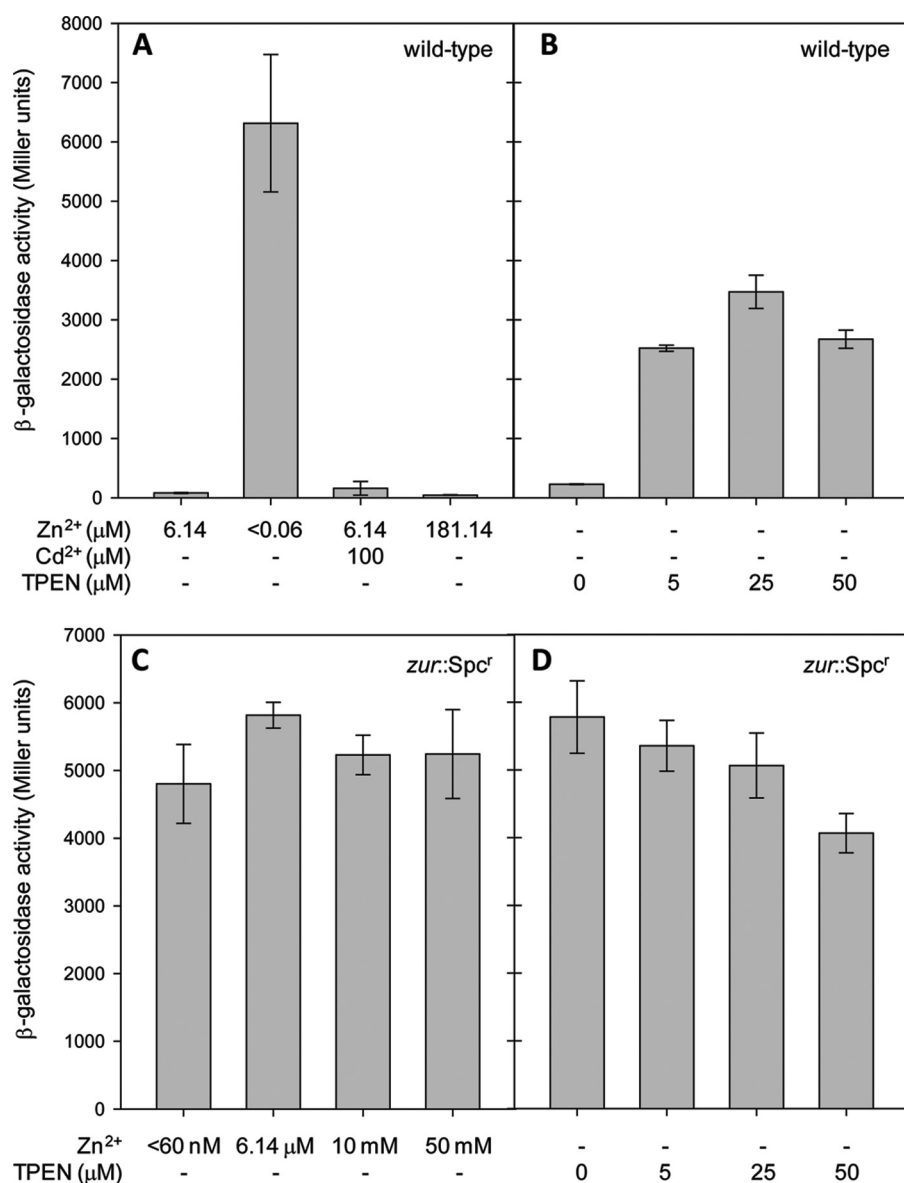


**FIGURE 3.  $\beta$ -Galactosidase activity of  $\lambda\Phi(P_{zinT-lacZ})$  under various conditions.** A and B,  $\beta$ -galactosidase activity of  $\lambda\Phi(P_{zinT-lacZ})$  (strain AL6) grown in GGM containing the concentrations of Zn<sup>2+</sup>, Cd<sup>2+</sup>, and TPEN shown. The Zn<sup>2+</sup> concentrations can be interpreted as follows: 6.14  $\mu$ M is GGM in which the bulk elements were Chelex-100-treated and then trace elements containing Zn<sup>2+</sup> were added back; <0.06  $\mu$ M is GGM in which extreme precautions were taken to exclude Zn<sup>2+</sup> (see text). The cultures were harvested when the A<sub>600</sub> reached 0.2–0.4. The means  $\pm$  standard deviation for three technical replicates are shown. The same results were seen on at least one other occasion. C and D,  $\beta$ -galactosidase activity of  $\lambda\Phi(P_{zinT-lacZ})$  in a *zur::Spcf* background (strain RKP5475) grown in GGM containing the Zn<sup>2+</sup> and TPEN concentrations shown. The cultures were harvested when the A<sub>600</sub> reached 0.2–0.4. The means and standard deviations of three technical replicates are shown. The same results were seen on at least one other occasion.

ments were carried out in triplicate, and similar results were seen on at least two separate occasions. We confirmed by qRT-PCR that the genes downstream of *ykgM*, *zinT*, and *znuA* (i.e. *ykgO*, *yodB* and *yebA*, respectively) were in all cases transcribed in the mutant strains.

We measured cellular Zn<sup>2+</sup> levels in bacteria grown in conditions of severe Zn<sup>2+</sup> limitation in batch culture. The levels of Zn<sup>2+</sup> detected in cell digests on analysis by ICP-AES were exceedingly low. Nevertheless, the *zinT::cam* strain contained ~9-fold less cellular Zn<sup>2+</sup> when cultured under Zn<sup>2+</sup> limitation (1.28  $\times 10^{-6}$  mg of Zn<sup>2+</sup>/mg of cells) than when grown in Zn<sup>2+</sup>-replete (1.16  $\times 10^{-5}$  mg of Zn<sup>2+</sup>/mg of cells) conditions.

Also, under Zn<sup>2+</sup>-deficient conditions, the *zinT::cam* strain contained nearly 3-fold less cellular Zn<sup>2+</sup> than MG1655 wild-type cells grown under similar conditions (1.28  $\times 10^{-6}$  mg of Zn<sup>2+</sup>/mg of cells and 3.40  $\times 10^{-6}$  mg of Zn<sup>2+</sup>/mg of cells, respectively). These data are the first to demonstrate a role for ZinT in Zn<sup>2+</sup> acquisition under strictly Zn<sup>2+</sup>-limited conditions. When the *znuA::kan* mutant was assayed after growth in Zn<sup>2+</sup>-depleted conditions, the measurement of cellular Zn<sup>2+</sup> was below the LOD. Similar results were seen on at least one other occasion.

**Transcriptional Regulation of *zinT* under Various Zn<sup>2+</sup> Concentrations**—Having established that *zinT* transcription was elevated on Zn<sup>2+</sup> depletion, a  $P_{zinT-lacZ}$  transcriptional fusion (25), in which *lacZ* is transcribed from the *zinT* promoter, was used to investigate an alternative Zn<sup>2+</sup> removal method and the effects of added Cd<sup>2+</sup> and Zn<sup>2+</sup>. Fig. 3A shows that  $\lambda\Phi(P_{zinT-lacZ})$  activity was highly up-regulated under the Zn<sup>2+</sup>-deficient conditions created here (in which Zn<sup>2+</sup> is excluded from the medium). These data were compared with cultures treated with TPEN (Fig. 3B), which is widely used as a Zn<sup>2+</sup> chelator (3, 7, 32, 42, 43, 45). Fig. 3B shows that expression from  $\lambda\Phi(P_{zinT-lacZ})$  increases with increasing TPEN concentrations in the growth medium. Although expression from  $\lambda\Phi(P_{zinT-lacZ})$  was higher in cells grown in medium containing TPEN than in cells grown in adequate Zn<sup>2+</sup>, it was lower than that of cells grown in medium from which Zn<sup>2+</sup>

has been rigorously eliminated (Fig. 3A). In LB medium, the  $P_{zinT-lacZ}$  fusion strain has previously been shown to respond to elevated levels of Cd<sup>2+</sup> but not of Zn<sup>2+</sup> (25). In GGM, the construct was again unresponsive to elevated Zn<sup>2+</sup>, but no response was seen to elevated Cd<sup>2+</sup> (Fig. 3A), although this may be due to difficulties in growing cells at high levels of Cd<sup>2+</sup>, which were near its maximum permissive concentration.

A Zur-binding site has been reported in the *zinT* promoter (41), and Zn<sup>2+</sup>-bound Zur represses the transcription of *znuABC* (8). Therefore, to test the hypothesis that Zur also negatively regulates *zinT*,  $\lambda\Phi(P_{zinT-lacZ})$  activity was monitored in a strain lacking *zur*. Fig. 3 (C and D) shows that, in a *zur* mutant,



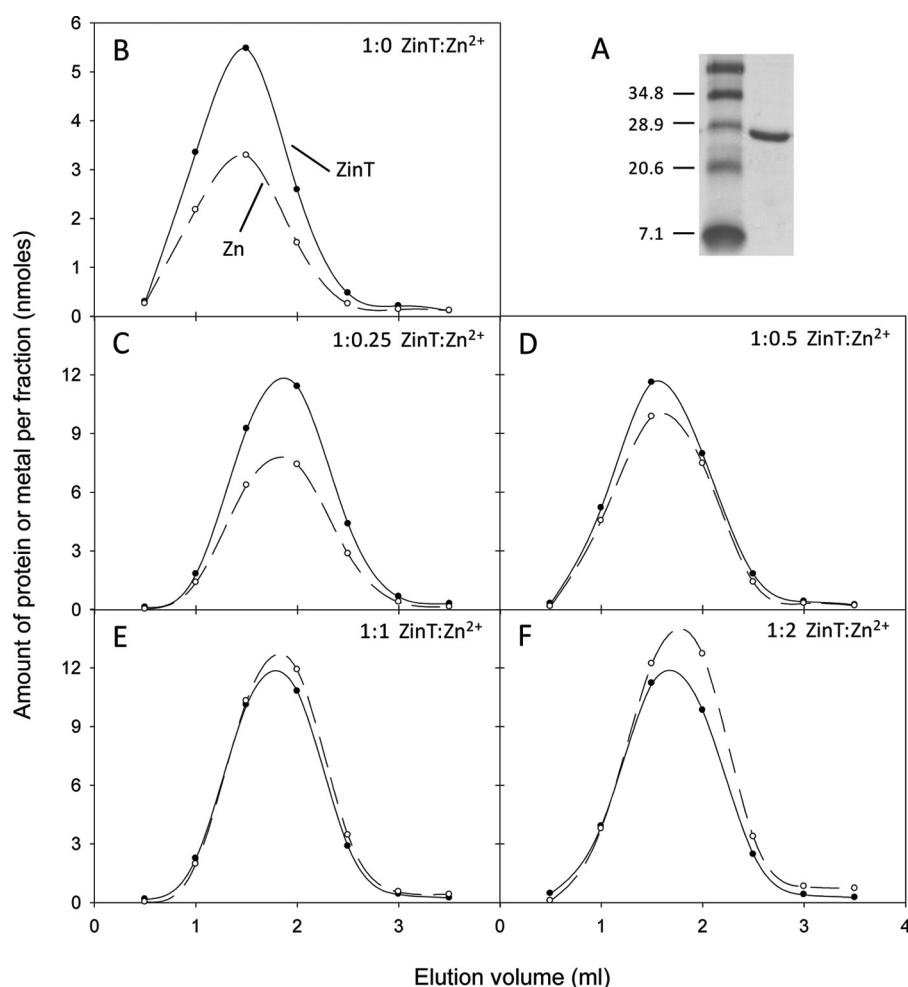


FIGURE 4. **Metal binding to purified ZinT.** *A*, purified recombinant ZinT (right lane) on an SDS-PAGE gel. Size markers (left lane) are shown in kDa. The elution profiles of ZinT and  $Zn^{2+}$  are from a PD-10 column following incubation of protein and metal ions. *B*, elution following incubation of 13.3 nmol of ZinT with no added metal. *C–F*, elution following incubation of 28.6 nmol of ZinT with 0.25, 0.5, 1, or 2 molar equivalents of  $Zn^{2+}$ . Filled circles with solid line, ZinT; open circles with dashed line,  $Zn^{2+}$ .

$\lambda\Phi(P_{zinT-lacZ})$  activity was not dependent on the extracellular  $Zn^{2+}$  concentration under any condition tested. Thus, Zur is a negative regulator of *zinT* transcription.

**Stoichiometric Binding of  $Zn^{2+}$  and  $Cd^{2+}$  by ZinT**—To investigate the possible role of ZinT in metal binding as suggested by the transcription and growth studies reported here, the *zinT* gene was cloned into pET28a such that the translated protein lacked the periplasmic signal sequence but was fused to a polyhistidine tag and thrombin cleavage site to aid purification. The polyhistidine tag was removed by cleavage with thrombin to minimize the danger of the protein adopting aberrant conformations. The sequence of the resultant protein, which was used to calculate the extinction coefficient, mimics the form of the protein found in the periplasm. Residual imidazole in the final ZinT preparation was avoided by using only a single wash step containing imidazole (20 mM) during purification and exchange into a buffer lacking imidazole before final use. The effective removal of the polyhistidine tag was confirmed by N-terminal sequencing. The pure recombinant protein (Fig. 4A) was incubated with different molar ratios of  $Zn^{2+}$  and then subjected to size exclusion chromatography to assess

co-elution of  $Zn^{2+}$  with ZinT. Fig. 4 shows the elution profiles of ZinT and  $Zn^{2+}$  following incubation of ZinT with 0, 0.25, 0.5, 1, and 2 molar equivalents of  $Zn^{2+}$ . Fig. 4B (and Fig. 5, A–D) shows that, even when no  $Zn^{2+}$  is added, ZinT co-eluted from the size exclusion column with  $Zn^{2+}$ . The occupancy of  $Zn^{2+}$  observed under these conditions (0.6 mol of  $Zn^{2+}$ /mol of ZinT) was approximately half that observed at superstoichiometric  $Zn^{2+}$ /ZinT ratios (Fig. 4F), and so we conclude that the  $Zn^{2+}$  content shown in Fig. 4B represents  $\sim 0.5$   $Zn^{2+}$ /ZinT. This suggests a high affinity of ZinT for  $Zn^{2+}$  and is reminiscent of the crystallization of ZinT (38); crystals formed in the absence of added metals contained  $Zn^{2+}$  or  $Ni^{2+}$ , indicative of high metal affinity (see “Discussion”). When ZinT was incubated with 0.25 or 0.5 molar equivalents of  $Zn^{2+}$  (Fig. 4, C and D) more  $Zn^{2+}$  co-eluted with ZinT than was originally added. However, when 1 (Fig. 4E), 2 (Fig. 4F), or 3 (data not shown) molar equivalents  $Zn^{2+}$  were incubated with ZinT, approximately one equivalent eluted from the column with the protein. These data provide evidence that ZinT binds one  $Zn^{2+}$  ion with high affinity.

Previous work (38) has suggested that ZinT is able to bind  $Cd^{2+}$ , and so the experiment was also carried out using  $Cd^{2+}$ . ZinT co-elutes from a size exclusion column with up to 1 molar equivalent of  $Cd^{2+}$ , even when initially incubated with more (Fig. 5, A–D). When 13.3 nmol of ZinT was incubated without  $Cd^{2+}$  prior to size exclusion chromatography, the eluate contained less than 18 pmol of  $Cd^{2+}$ /fraction (not shown). It should be noted that, in the case of  $Cd^{2+}$ , the  $Cd^{2+}$ /ZinT ratio was  $\sim 0.9$  but never exceeded 1 (Fig. 5D) unlike the case with  $Zn^{2+}$  (Fig. 4F). This is attributable to the inevitable contamination of reagents and materials with  $Zn^{2+}$  but not  $Cd^{2+}$ .

To investigate competition of  $Zn^{2+}$  and  $Cd^{2+}$  for site(s) in ZinT, the protein was incubated with both metals, and co-elution of metals and protein was assayed. ZinT co-eluted with almost 1 molar equivalent of  $Zn^{2+}$  and  $\sim 0.5$  molar equivalents of  $Cd^{2+}$  (Fig. 5E). These ratios were similar when the  $Cd^{2+}$ : $Zn^{2+}$  ratio was increased to 2:1 (Fig. 5F), indicating that ZinT preferentially binds  $Zn^{2+}$  over  $Cd^{2+}$ . Multi-element analysis of the eluate also revealed  $\sim 0.5$  molar equivalents of  $Co^{2+}$  with ZinT. This was seen in all experiments, and the reasons for this are discussed below. Two metal ions/ZinT protein would match previous structural data (38).

## Transcriptional Response to Zinc Limitation

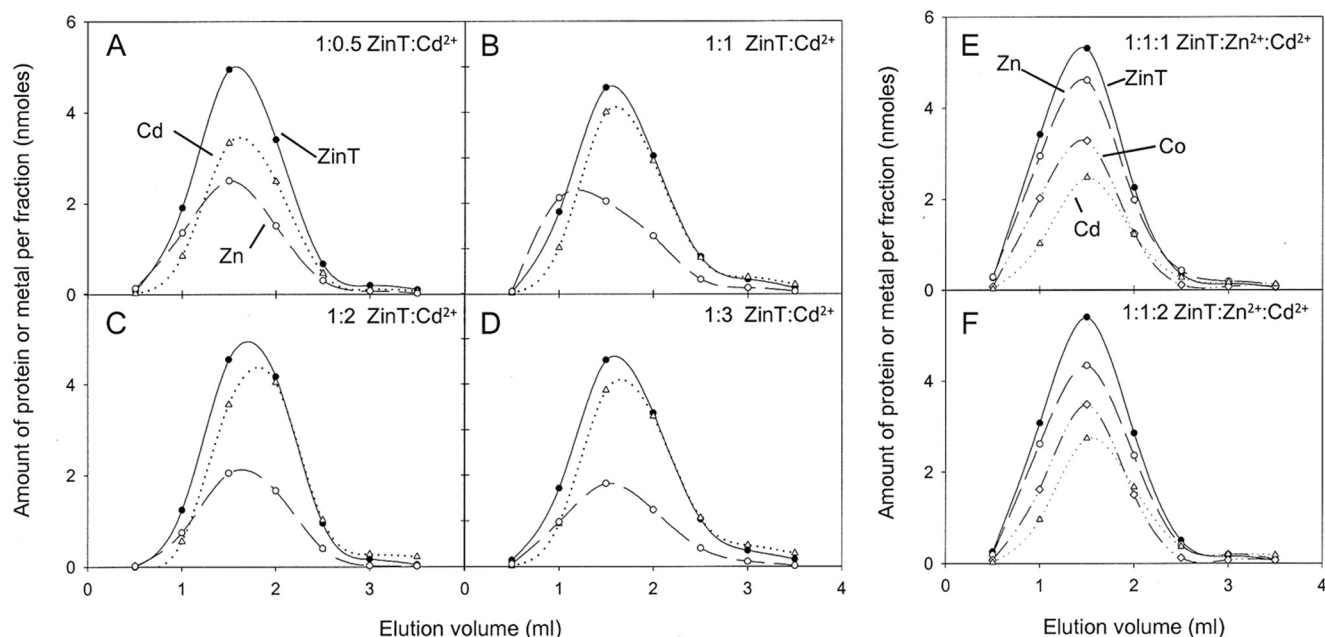


FIGURE 5. Elution profiles of ZnT,  $Zn^{2+}$ , and  $Cd^{2+}$  from a PD-10 column following incubation of protein and metal ions. A–D, elution following incubation of 17.8 nmol of ZnT with 0.5, 1, 2, or 3 molar equivalents of  $Cd^{2+}$ . Filled circles with solid line, ZnT; open circles with dashed line,  $Zn^{2+}$ ; open triangles with dotted line,  $Cd^{2+}$ . E and F, elution following incubation of 13.3 nmol of ZnT with 1 molar equivalent of  $Zn^{2+}$  and 1 molar equivalent of  $Cd^{2+}$  or with 1 molar equivalent of  $Zn^{2+}$  and two molar equivalents of  $Cd^{2+}$ . Filled circles with solid line, ZnT; open circles with dashed line,  $Zn^{2+}$ ; open diamonds with dotted and dashed line,  $Co^{2+}$ ; open triangles with dotted line,  $Cd^{2+}$ .

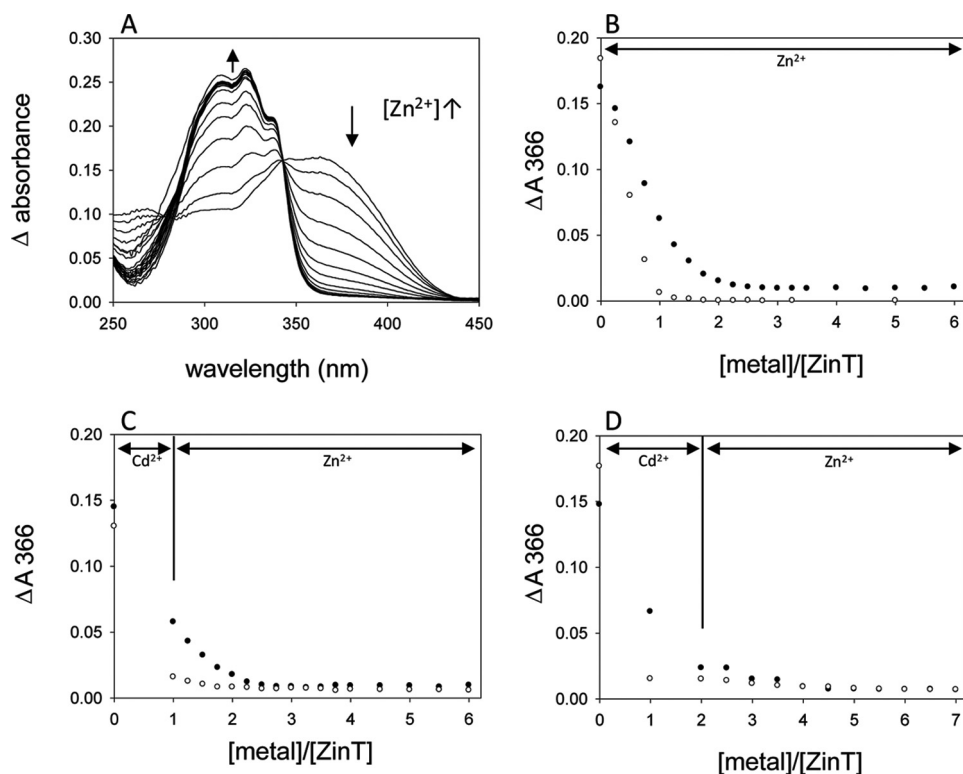


FIGURE 6. Titration of ZnT and/or MF with  $Zn^{2+}$  and/or  $Cd^{2+}$ . A, representative difference spectra (*i.e.* minus the protein-only spectrum) of a titration of 14.5  $\mu M$  ZnT and 14.5  $\mu M$  MF with  $Zn^{2+}$  (0.25–3.5 molar equivalents  $Zn^{2+}$  in 0.25 steps and then 4–6 molar equivalents in 0.5 steps). The arrows indicate the direction of absorbance changes as  $Zn^{2+}$  is added. B, titration of 14.5  $\mu M$  ZnT and 14.5  $\mu M$  MF with  $Zn^{2+}$ . C, titration of 14.3  $\mu M$  ZnT and 14.3  $\mu M$  MF with 1 molar equivalent of  $Cd^{2+}$ , then  $Zn^{2+}$  in 0.5 molar equivalent steps to 4 molar equivalents and then  $Zn^{2+}$  in 0.5 molar equivalent steps to 6 molar equivalents. D, titration of 14.1  $\mu M$  ZnT and 14.1  $\mu M$  MF with 2 molar equivalents of  $Cd^{2+}$  and then  $Zn^{2+}$  in 0.5 molar equivalent steps. In B–D, absorbance change at 366 nm is plotted against molar equivalents of metal added. The filled circles are in the presence of ZnT; open circles are in the absence of ZnT (MF and buffer only). The lines indicate whether the added metal was  $Zn^{2+}$  or  $Cd^{2+}$ .

*Mag-fura-2 (MF) and ZnT Competitive Metal Binding*—To estimate the affinity of ZnT for  $Zn^{2+}$ , Mag-fura-2, a chromophore that binds  $Zn^{2+}$  in a 1:1 ratio (46) and with a  $K_d$  of 20 nM (47), was used. Its absorption maximum shifts from 366 to 325 nm on  $Zn^{2+}$  binding, which is accompanied by a decrease in its extinction coefficient from 29,900  $M^{-1} cm^{-1}$  (MF) to 1880  $M^{-1} cm^{-1}$  ( $Zn^{2+}$ -MF) (46). Therefore  $Zn^{2+}$  binding to MF can be tracked by examining the absorbance at 366 nm (Fig. 6A). Fig. 6B shows a titration of a 1:1 ZnT:MF mixture (filled circles) and MF alone (open circles) with  $Zn^{2+}$ . When ZnT was not present, the  $\Delta A_{366}$  decreased to zero when 1 molar equivalent of  $Zn^{2+}$  had been added. When ZnT was present, however, incremental additions of  $Zn^{2+}$  gave smaller decreases in MF absorbance reaching a plateau at 2 molar equivalents of  $Zn^{2+}$ . This provides good evidence that, although the affinity of ZnT for  $Zn^{2+}$  is not high enough to completely outstrip MF of  $Zn^{2+}$ , ZnT competes with MF for binding of  $Zn^{2+}$ . The

$K_d$  for  $Zn^{2+}$  binding by ZinT is therefore not less than 20 nM, but of an order that is able to compete with MF for  $Zn^{2+}$ .

MF also binds  $Cd^{2+}$  in a 1:1 ratio and has a  $K_d$  for  $Cd^{2+}$  of 126 nM (48). The addition of  $Cd^{2+}$  to MF and ZinT (Fig. 6, C and D) elicited a smaller decrease in absorbance than with MF alone, again indicating the ability of ZinT to compete with MF for  $Cd^{2+}$ . Without protein, the decrease in absorbance at 366 nm plateaued at 1 molar equivalent of metal added, whereas when ZinT was present, this shifted to 2. These data together suggest that ZinT has one binding site for metal that can be occupied by  $Cd^{2+}$  or  $Zn^{2+}$  and that the site has a sufficiently low  $K_d$  to be able to compete with MF for these metals.

## DISCUSSION

The manipulation of metal ion concentrations in biological systems, so that the consequences of metal excess and limitation may be studied, is a major challenge. Global responses to elevated levels of  $Ag^{2+}$ ,  $Cd^{2+}$ ,  $Cu^{2+}$ ,  $Ni^{2+}$ ,  $Zn^{2+}$ , and arsenic (14, 49–54) have been reported. However, constituents of complex growth medium can bind to metal ions and result in the metal ion concentration available to the cells being orders of magnitude lower than that added (16). For the first time, we have grown  $Zn^{2+}$ -depleted *E. coli* in batch and chemostat culture in defined medium, without recourse to chelating agents, and defined the transcriptome associated with severe  $Zn^{2+}$  limitation. In batch culture, wild-type *E. coli* MG1655 cells grown in  $Zn^{2+}$ -depleted cultures showed an increased doubling time (Fig. 1A) and a reduction in  $Zn^{2+}$  content compared with  $Zn^{2+}$ -replete cultures. Thus, in the face of extreme  $Zn^{2+}$  depletion in the extracellular medium, homeostatic mechanisms ensure adequate cellular zinc contents.

$Zn^{2+}$ -depleted medium was successfully prepared by eliminating  $Zn^{2+}$  during medium preparation and culture. In contrast, chelators can be unspecific, strip metals from exposed sites and increase the availability of certain metals (16). The major disadvantage of using chelators is that the metal is still present in the medium to be picked up by proteins with a higher affinity for the metal than that exhibited by the chelator. For example, ZnuA is able to compete with EDTA for  $Zn^{2+}$  (6). Fig. 3A highlights the disadvantage of using chelators to study  $Zn^{2+}$  deficiency; the widely used chelator TPEN was less effective than  $Zn^{2+}$  elimination, as judged by  $\lambda\Phi(P_{zinT-lacZ})$  activity. Although neither are specific to  $Zn^{2+}$ , both TPEN and EDTA have been used in studies focusing on  $Zn^{2+}$  depletion (see earlier references and Ref. 55).

Fig. 2 and Table 3 show that cells grown in  $Zn^{2+}$ -depleted medium accumulate  $Zn^{2+}$  that cannot be accounted for by the medium constituents. Table 3 shows that the extent of leaching decreased with successive experiments in the same chemostat apparatus. The most likely explanation is that metal is actively leached from the glassware (flasks or chemostat vessel). Kay (29) notes that acid washing removes only surface  $Zn^{2+}$ , which can be replaced from deeper within the glass. Previous studies have shown that growing cells in medium deficient in one nutrient can lead to cells evolving mechanisms to increase the uptake of that nutrient (56).

In contrast to Ref. 10, this study found only nine genes to be differentially regulated in response to  $Zn^{2+}$  starvation after careful metal avoidance and extraction. The small number of differentially regulated genes suggests that, because of the ubiquity of  $Zn^{2+}$  in the environment, the cells have not evolved elaborate mechanisms to cope with extreme  $Zn^{2+}$  deficiency. Interestingly, computational analysis found only three candidate Zur sites in the *E. coli* genome, and these sites were immediately upstream of three genes identified here: *zinT*, *ykgM*, and *znuA* (41).

There is a precedent in *Bacillus* for redistribution of  $Zn^{2+}$  under conditions of  $Zn^{2+}$  starvation, involving the synthesis of non- $Zn^{2+}$  finger homologues of  $Zn^{2+}$ -binding ribosomal proteins. Makarova *et al.* (57) searched sequenced genomes and found that genes encoding some ribosomal proteins were present as two copies: one, designated  $C^+$ , containing a  $Zn^{2+}$ -binding motif and a second, designated  $C^-$ , in which this motif is missing. In the case of the *E. coli* ribosomal protein L31, the  $C^+$  form is encoded by *rpmE* and the  $C^-$  form by *ykgM* (41) identified in the present study. Based on the present results, we hypothesize that non- $Zn^{2+}$ -containing L31 proteins displace the  $Zn^{2+}$ -containing form in ribosomes, and subsequent degradation of the latter form would release  $Zn^{2+}$  for use by other proteins. The number of ribosomes in the cell would make this a significant  $Zn^{2+}$  reserve. Such a model has been experimentally proven for L31 proteins in *Bacillus subtilis* (58, 59) and *Streptomyces coelicolor* (60, 61).

The present study shows that *zinT* expression is increased most dramatically, not by  $Cd^{2+}$  addition as reported previously (27), but by  $Zn^{2+}$  removal. However, the present and past findings are reconciled by the fact that  $Cd^{2+}$  may displace other metals from enzymes, such as  $Zn^{2+}$  from alkaline phosphatase in *E. coli* (2, 25), so that  $Cd^{2+}$  exposure mimics  $Zn^{2+}$  depletion. Panina *et al.* (41) reported a Zur-binding site in the *zinT* promoter. Monitoring expression from  $\lambda\Phi(P_{zinT-lacZ})$  in a strain lacking *zur* showed constitutive de-repression, regardless of extracellular  $Zn^{2+}$  concentration, confirming that Zur is involved in the regulation of *zinT* (Fig. 3). This was also reported in an unpublished thesis cited in a review (62).

Based on the established link between ZinT and  $Cd^{2+}$ , David *et al.* (38) included the metal (20 mM) in crystallization trials and obtained a crystal form distinct from that obtained under crystallization conditions that included 200 mM  $Zn^{2+}$  or no added metal. The crystal structure reveals a principal metal-binding site (common to all crystallized forms) that binds one  $Cd^{2+}$  or two  $Zn^{2+}$  ions. Further metal ions are found at the protein surface at intermolecular, negatively charged sites formed by residues from neighboring ZinT molecules. The crystal form prepared in the absence of exogenous metal also revealed one metal ion bound in the central, common, metal-binding site; this metal was positioned similarly to  $Cd^{2+}$  and coordinated by the three same His residues. The buried metal-binding site must be of high affinity, because no divalent cations were included in crystallization of the native form. The binding geometry suggests that the metal in the native form is  $Zn^{2+}$ , although contamination by  $Ni^{2+}$  from the affinity chromatography or other metal ions could not be excluded, and x-ray fluorescence suggested the presence of  $Ni^{2+}$ , albeit in an

## Transcriptional Response to Zinc Limitation

unusual distorted tetrahedral geometry. Fig. 5 (*E* and *F*) shows that, in our hands,  $\sim 0.5$  molar equivalents  $\text{Co}^{2+}$  co-elute with the ZinT protein. It is likely that this  $\text{Co}^{2+}$  has been picked up from the TALON column used during purification, again providing evidence for a high affinity metal-binding site within ZinT. No  $\text{Ni}^{2+}$  was found in eluting samples (data not shown).

On the basis of the crystallography, David *et al.* (38) could not conclude which metal would bind to ZinT under physiological conditions. The present study shows clearly that ZinT binds both  $\text{Zn}^{2+}$  and  $\text{Cd}^{2+}$  with high affinity. The direct binding experiments (Fig. 5, *E* and *F*) show that more  $\text{Zn}^{2+}$  remains bound to ZinT after size exclusion chromatography than  $\text{Cd}^{2+}$ , providing evidence that  $\text{Zn}^{2+}$  binds to ZinT more tightly than  $\text{Cd}^{2+}$ . Also, the  $K_d$  of MF for  $\text{Cd}^{2+}$  is greater than for  $\text{Zn}^{2+}$ , so somewhat weaker binding by  $\text{Cd}^{2+}$  would not be detected in the Mag-Fura-2 competition experiments. Fig. 5 (*E* and *F*) shows that more than 1 molar equivalent of metal can bind to the protein. This is consistent with the crystal structure proposed by David *et al.* (38), which suggests that at least two  $\text{Zn}^{2+}$  ions can bind in the vicinity of the high affinity site, and that there is additional capacity for further  $\text{Zn}^{2+}$ , up to 4, although this may be due to intermolecular contacts formed during crystallization. The finding that one  $\text{Zn}^{2+}$  ion is needed to saturate the protein, as assessed by competition with Mag-Fura-2, is entirely consistent with the crystallographic data because this experiment can only report on metal binding to ZinT that is tighter than 20 nM. Although this site in ZinT accommodates different metal ions, the marked accumulation of *zinT* mRNA by extreme  $\text{Zn}^{2+}$  limitation strongly suggests that the physiological role of ZinT is ferrying  $\text{Zn}^{2+}$  ions in the periplasm. Indeed, David *et al.* (38) suggested that the binding of a second metal, possibly at a lower affinity site, could trigger a conformational change that promotes transport across the membrane or interaction with an unidentified ABC-type transporter. In support of this is the fact that ZinT shows sequence similarity to a number of periplasmic metal-binding receptors of ABC metal transport systems that have been shown to bind  $\text{Zn}^{2+}$ .

In a recent paper (9), growth in media with various  $\text{Zn}^{2+}$  supplements, or none, was purported to show "dependence of the  $\Delta zinT$  mutant strain on zinc for growth."  $\text{Zn}^{2+}$ -limited conditions were those in which reduced growth yields ( $A_{595}$ ) were observed relative to growth at 0.6–1 mM added  $\text{Zn}^{2+}$ . In defined medium containing less than 0.4 mM  $\text{Zn}^{2+}$ , the mutant grew to lower  $A$  levels after 10 h than the wild type, but at high  $\text{Zn}^{2+}$  (0.6–1 mM), the *zinT* mutant grew to higher  $A$  values than the wild-type strain. This is in conflict with the present work (Fig. 1, *A* and *C*), which shows that the *zinT* mutant and wild-type strains grew similarly, even at only 60 nM  $\text{Zn}^{2+}$ . Surprisingly, Kershaw *et al.* (9) also found that even growth of the wild-type strain was impaired at low  $\text{Zn}^{2+}$  concentrations (0.4, 0.05 mM added  $\text{Zn}^{2+}$ ); with no added  $\text{Zn}^{2+}$ , growth was barely detectable. The claim that *E. coli* shows a strict dependence on added  $\text{Zn}^{2+}$  is, to our knowledge, unprecedented in the literature. Considerations of biomass composition suggest that the  $\text{Zn}^{2+}$  concentration in the medium used by Kershaw *et al.* (9) (0.5 mg liter<sup>-1</sup>) should support growth to a yield of 2.5 g of dry weight liter<sup>-1</sup> (17), well in excess of the  $A_{595}$  of  $\sim 0.5$  or lower reported (9). Furthermore, inspection of the responses of both

wild-type and *zinT* mutant strains to metals reveals that the experiments (9) to define the  $\text{Zn}^{2+}$  response were conducted at limiting copper concentrations; the basic defined medium contained 0.62  $\mu\text{M}$  copper (0.1 mg  $\text{CuSO}_4$  liter<sup>-1</sup>),  $\sim 1000$ -fold lower than the required copper concentration for optimal growth of both strains. Similarly, experiments to define the copper response were conducted at limiting  $\text{Zn}^{2+}$  concentrations; the basic defined medium contained 3.1  $\mu\text{M}$   $\text{Zn}^{2+}$  (0.5 mg  $\text{ZnSO}_4$  liter<sup>-1</sup>), *i.e.* much lower than the concentration at which both strains showed reduced cell yield. These calculations may explain why the cell yields at saturating copper concentrations (0.6–1.0 mM) were significantly lower than those at saturating  $\text{Zn}^{2+}$  concentrations (0.6–1.0 mM). Thus, the data of Kershaw *et al.* (9) do not provide robust evidence that the *zinT* mutant shows a growth disadvantage at low  $\text{Zn}^{2+}$  ion concentrations and conflict with previous work demonstrating the exceedingly low copper concentrations required for Cu-limited growth (3, 63).

Kershaw *et al.* (9) reported that ZinT binds metal ions.  $\text{Cd}^{2+}$  binding was observed when  $\text{Cd}^{2+}$  was incubated with the protein in a 1:1 ratio (0.1 mM ZinT:0.1 mM  $\text{Cd}^{2+}$ ), although the resolution of a peak corresponding to mass 22,450 (ZinT plus 1  $\text{Cd}^{2+}$ ) is poor. The mass of the ZinT-Cd peak varied by 2 Da (as did the mass of apo-ZinT). The authors were only able to detect binding of  $\text{Zn}^{2+}$  to ZinT when 5 or more molar equivalents were added, although their other experiments detected binding when ZinT was incubated with less than 0.1 molar equivalent of  $\text{Zn}^{2+}$ . In Figs. 4 and 5 of the present study, we show binding of  $\text{Zn}^{2+}$  to ZinT when no metal is added because of the high affinity of ZinT for contaminating  $\text{Zn}^{2+}$  in the buffers.

In addition to the need to sense  $\text{Zn}^{2+}$  levels to maintain homeostasis for all cellular systems, the lack of  $\text{Zn}^{2+}$  may be sensed by pathogens as indicative of entry into the host and thus trigger expression of virulence factors. Indeed, several studies in different bacteria have established that ZnuA or ZnuABC (or homologues) are required for bacterial replication in the infected host (see Refs. 44 and 55, among others).

In conclusion, we propose that, when cells are severely starved of  $\text{Zn}^{2+}$ , the response is to increase  $\text{Zn}^{2+}$  uptake into the cell and redistribute nonessential  $\text{Zn}^{2+}$ . The *rpmE* gene expresses the  $\text{Zn}^{2+}$  finger L31 protein that is incorporated into the ribosome. Upon  $\text{Zn}^{2+}$  depletion, the *ykgM*-encoded L31 protein is expressed (probably de-repressed by Zur) and becomes preferentially bound to the ribosome (the exact mechanism is unclear), allowing  $\text{Zn}^{2+}$  within the *rpmE*-encoded L31 to be recycled. The physiological role of ZinT remains to be fully established, but it may function as a  $\text{Zn}^{2+}$  chaperone to the membrane-bound  $\text{Zn}^{2+}$  importer ZnuBC (or a different importer) or mediate direct transport from the periplasm to the cytoplasm.  $\text{Zn}^{2+}$  is the metal that binds most tightly. This study provides a new appreciation of the regulation of *zinT* and the role of ZinT in protecting cells from  $\text{Zn}^{2+}$  depletion.

---

*Acknowledgment*—We thank Dr. A. J. G. Moir (Krebs Institute Sequencing and Synthesis Facility, University of Sheffield, Sheffield, United Kingdom) for carrying out the N-terminal protein sequencing.

---

## REFERENCES

- Berg, J. M., and Shi, Y. (1996) *Science* **271**, 1081–1085
- Fraústo da Silva, J. J. R., and Williams, R. J. P. (2001) *The Biological Chemistry of the Elements: The Inorganic Chemistry of Life*, Oxford University Press, Oxford
- Outten, C. E., and O'Halloran, T. V. (2001) *Science* **292**, 2488–2492
- Andreini, C., Banci, L., Bertini, I., and Rosato, A. (2006) *J Proteome Res* **5**, 3173–3178
- Blencowe, D. K., and Morby, A. P. (2003) *FEMS Microbiol. Rev.* **27**, 291–311
- Berducci, G., Mazzetti, A. P., Rotilio, G., and Battistoni, A. (2004) *FEBS Lett.* **569**, 289–292
- Patzer, S. I., and Hantke, K. (1998) *Mol. Microbiol.* **28**, 1199–1210
- Patzer, S. I., and Hantke, K. (2000) *J. Biol. Chem.* **275**, 24321–24332
- Kershaw, C. J., Brown, N. L., and Hobman, J. L. (2007) *Biochem. Biophys. Res. Commun.* **364**, 66–71
- Sigdel, T. K., Easton, J. A., and Crowder, M. W. (2006) *J. Bacteriol.* **188**, 6709–6713
- Hayes, A., Zhang, N., Wu, J., Butler, P. R., Hauser, N. C., Hoheisel, J. D., Lim, F. L., Sharrocks, A. D., and Oliver, S. G. (2002) *Methods* **26**, 281–290
- Hoskisson, P. A., and Hobbs, G. (2005) *Microbiology* **151**, 3153–3159
- Piper, M. D., Daran-Lapujade, P., Bro, C., Regenber, B., Knudsen, S., Nielsen, J., and Pronk, J. T. (2002) *J. Biol. Chem.* **277**, 37001–37008
- Lee, L. J., Barrett, J. A., and Poole, R. K. (2005) *J. Bacteriol.* **187**, 1124–1134
- Beard, S. J., Hashim, R., Membrillo-Hernández, J., Hughes, M. N., and Poole, R. K. (1997) *Mol. Microbiol.* **25**, 883–891
- Hughes, M. N., and Poole, R. K. (1991) *J. Gen. Microbiol.* **137**, 725–734
- Pirt, S. J. (1975) *Principles of Microbe and Cell Cultivation*, Blackwell Scientific Publications, Oxford
- Ferenci, T. (2008) *Adv. Microb. Physiol.* **53**, 169–229
- Garland, P. B., and Randle, P. J. (1962) *Nature* **196**, 987–988
- Cherny, R. A., Atwood, C. S., Xilinas, M. E., Gray, D. N., Jones, W. D., McLean, C. A., Barnham, K. J., Volitakis, I., Fraser, F. W., Kim, Y., Huang, X., Goldstein, L. E., Moir, R. D., Lim, J. T., Beyreuther, K., Zheng, H., Tanzi, R. E., Masters, C. L., and Bush, A. I. (2001) *Neuron* **30**, 665–676
- Lin, P. S., Kwock, L., Hefter, K., and Misslbeck, G. (1983) *Cancer Res.* **43**, 1049–1053
- Mukherjee, G., and Ghosh, T. (1995) *J. Inorg. Biochem.* **59**, 827–833
- Sebat, J. L., Paszczyński, A. J., Cortese, M. S., and Crawford, R. L. (2001) *Appl. Environ. Microbiol.* **67**, 3934–3942
- Datsenko, K. A., and Wanner, B. L. (2000) *Proc. Natl. Acad. Sci. U. S. A.* **97**, 6640–6645
- Puskárová, A., Ferienc, P., Kormanec, J., Homerová, D., Farewell, A., and Nyström, T. (2002) *Microbiology* **148**, 3801–3811
- Miller, J. H. (1972) *Experiments in Molecular Genetics*, Cold Spring Harbor Laboratory, Cold Spring Harbor, NY
- Ferienc, P., Farewell, A., and Nyström, T. (1998) *Microbiology* **144**, 1045–1050
- Gill, S. C., and von Hippel, P. H. (1989) *Anal. Biochem.* **182**, 319–326
- Kay, A. R. (2004) *BMC Physiol.* **4**, 4
- Koch, A. L. (1961) *Biochim. Biophys. Acta* **51**, 429–441
- Neidhardt, F. C., Ingraham, J. L., and Schaechter, M. (1990) *Physiology of the Bacterial Cell: A Molecular Approach*, pp. 418–441, Sinauer Associates, Inc., Sunderland, MA
- Jackson, K. A., Helston, R. M., McKay, J. A., O'Neill, E. D., Mathers, J. C., and Ford, D. (2007) *J. Biol. Chem.* **282**, 10423–10431
- Barrett, T., Troup, D. B., Wilhite, S. E., Ledoux, P., Rudnev, D., Evangelista, C., Kim, I. F., Soboleva, A., Tomashevsky, M., and Edgar, R. (2007) *Nucleic Acids Res.* **35**, D760–D765
- Laurent-Winter, C., Ngo, S., Danchin, A., and Bertin, P. (1997) *Eur. J. Biochem.* **244**, 767–773
- Birch, R. M., O'Byrne, C., Booth, I. R., and Cash, P. (2003) *Proteomics* **3**, 764–776
- Kannan, G., Wilks, J. C., Fitzgerald, D. M., Jones, B. D., Bondurant, S. S., and Slonczewski, J. L. (2008) *BMC Microbiol.* **8**, 37
- David, G., Blondeau, K., Renouard, M., and Lewit-Bentley, A. (2002) *Acta Crystallogr. D Biol. Crystallogr.* **58**, 1243–1245
- David, G., Blondeau, K., Schiltz, M., Penel, S., and Lewit-Bentley, A. (2003) *J. Biol. Chem.* **278**, 43728–43735
- Stojnev, T., Harichová, J., Ferienc, P., and Nyström, T. (2007) *Curr. Microbiol.* **55**, 99–104
- Kadokura, H., Tian, H., Zander, T., Bardwell, J. C., and Beckwith, J. (2004) *Science* **303**, 534–537
- Panina, E. M., Mironov, A. A., and Gelfand, M. S. (2003) *Proc. Natl. Acad. Sci. U. S. A.* **100**, 9912–9917
- Cai, F., Adrion, C. B., and Keller, J. E. (2006) *Infect. Immun.* **74**, 5617–5624
- Fekkes, P., de Wit, J. G., Boorsma, A., Friesen, R. H., and Driessen, A. J. (1999) *Biochemistry* **38**, 5111–5116
- Ammendola, S., Pasquali, P., Pistoia, C., Petrucci, P., Petrarca, P., Rotilio, G., and Battistoni, A. (2007) *Infect. Immun.* **75**, 5867–5876
- Scott, C., Rawsthorne, H., Upadhyay, M., Shearman, C. A., Gasson, M. J., Guest, J. R., and Green, J. (2000) *FEMS Microbiol. Lett.* **192**, 85–89
- Yatsunyk, L. A., Easton, J. A., Kim, L. R., Sugarbaker, S. A., Bennett, B., Breece, R. M., Vorontsov, I., Tierney, D. L., Crowder, M. W., and Rosenzweig, A. C. (2008) *J. Biol. Inorg. Chem.* **13**, 271–288
- Simons, T. J. (1993) *J. Biochem. Biophys. Methods* **27**, 25–37
- de Seny, D., Heinz, U., Wommer, S., Kiefer, M., Meyer-Klaucke, W., Galeni, M., Frere, J. M., Bauer, R., and Adolph, H. W. (2001) *J. Biol. Chem.* **276**, 45065–45078
- Brocklehurst, K. R., and Morby, A. P. (2000) *Microbiology* **146**, 2277–2282
- Kershaw, C. J., Brown, N. L., Constantinidou, C., Patel, M. D., and Hobman, J. L. (2005) *Microbiology* **151**, 1187–1198
- Moore, C. M., Gaballa, A., Hui, M., Ye, R. W., and Helmann, J. D. (2005) *Mol. Microbiol.* **57**, 27–40
- Wang, A., and Crowley, D. E. (2005) *J. Bacteriol.* **187**, 3259–3266
- Yamamoto, K., and Ishihama, A. (2005) *Mol. Microbiol.* **56**, 215–227
- Yamamoto, K., and Ishihama, A. (2005) *J. Bacteriol.* **187**, 6333–6340
- Davis, L. M., Kakuda, T., and DiRita, V. J. (2009) *J. Bacteriol.* **191**, 1631–1640
- Notley-McRobb, L., and Ferenci, T. (1999) *Environ. Microbiol.* **1**, 45–52
- Makarova, K. S., Ponomarev, V. A., and Koonin, E. V. (2001) *Genome Biol.* **2**, research 0033.1–0033.14
- Akanuma, G., Nanamiya, H., Natori, Y., Nomura, N., and Kawamura, F. (2006) *J. Bacteriol.* **188**, 2715–2720
- Nanamiya, H., Akanuma, G., Natori, Y., Murayama, R., Kosono, S., Kudo, T., Kobayashi, K., Ogasawara, N., Park, S. M., Ochi, K., and Kawamura, F. (2004) *Mol. Microbiol.* **52**, 273–283
- Owen, G. A., Pascoe, B., Kallifidas, D., and Paget, M. S. (2007) *J. Bacteriol.* **189**, 4078–4086
- Shin, J. H., Oh, S. Y., Kim, S. J., and Roe, J. H. (2007) *J. Bacteriol.* **189**, 4070–4077
- Hantke, K. (2005) *Curr. Opin. Microbiol.* **8**, 196–202
- Ciccognani, D. T., Hughes, M. N., and Poole, R. K. (1992) *FEMS Microbiol. Lett.* **73**, 1–6